Verisig: verifying safety properties of hybrid systems with neural network controllers

Radoslav Ivanov, James Weimer, Rajeev Alur, George J. Pappas, Insup Lee University of Pennsylvania Philadelphia, Pennsylvania {rivanov,weimerj,alur,pappasg,lee}@seas.upenn.edu

ABSTRACT

This paper presents Verisig, a hybrid system approach to verifying safety properties of closed-loop systems using neural networks as controllers. We focus on sigmoid-based networks and exploit the fact that the sigmoid is the solution to a quadratic differential equation, which allows us to transform the neural network into an equivalent hybrid system. By composing the network's hybrid system with the plant's, we transform the problem into a hybrid system verification problem which can be solved using state-of-theart reachability tools. We show that reachability is decidable for networks with one hidden layer and decidable for general networks if Schanuel's conjecture is true. We evaluate the applicability and scalability of Verisig in two case studies, one from reinforcement learning and one in which the neural network is used to approximate a model predictive controller.

CCS CONCEPTS

Theory of computation → Timed and hybrid models; • Software and its engineering → Formal methods; • Computing methodologies → Neural networks;

KEYWORDS

Neural Network Verification, Hybrid Systems with Neural Network Controllers, Learning-Enabled Components

ACM Reference Format:

Radoslav Ivanov, James Weimer, Rajeev Alur, George J. Pappas, Insup Lee. 2019. Verisig: verifying safety properties of hybrid systems with neural network controllers. In 22nd ACM International Conference on Hybrid Systems: Computation and Control (HSCC '19), April 16–18, 2019, Montreal, QC, Canada. ACM, New York, NY, USA, 10 pages. https://doi.org/10.1145/3302504.3311806

This material is based upon work supported by the Air Force Research Laboratory (AFRL) and the Defense Advanced Research Projects Agency (DARPA) under Contract No. FA8750-18-C-0090. Any opinions, findings and conclusions or recommendations expressed in this material are those of the author(s) and do not necessarily reflect the views of the AFRL, DARPA, the Department of Defense, or the United States Government. This work was supported in part by NSF grant CNS-1837244. This research was supported in part by ONR N000141712012.

Permission to make digital or hard copies of all or part of this work for personal or classroom use is granted without fee provided that copies are not made or distributed for profit or commercial advantage and that copies bear this notice and the full citation on the first page. Copyrights for components of this work owned by others than the author(s) must be honored. Abstracting with credit is permitted. To copy otherwise, or republish, to post on servers or to redistribute to lists, requires prior specific permission and/or a fee. Request permissions from permissions@acm.org.

HSCC '19, April 16-18, 2019, Montreal, OC, Canada

© 2019 Copyright held by the owner/author(s). Publication rights licensed to ACM. ACM ISBN 978-1-4503-6282-5/19/04...\$15.00 https://doi.org/10.1145/3302504.3311806

1 INTRODUCTION

In recent years, deep neural networks (DNNs) have been successfully applied to multiple challenging tasks such as image processing [29], reinforcement learning [20], learning model predictive controllers (MPCs) [26], and games such as Go [27]. These results have inspired system developers to use DNNs in safety-critical Cyber-Physical Systems (CPS) such as autonomous vehicles [3] and air traffic collision avoidance systems [14]. At the same time, several recent incidents (e.g., Tesla [1] and Uber [3] autonomous driving crashes) have underscored the need to better understand DNNs and verify safety properties about CPS using such networks.

The traditional way of assessing a learning algorithm's performance is through bounding the expected generalization error (EGE) of a trained classifier, i.e., the expected difference between the classifier's error on training versus test examples [21]. The EGE can be usually bounded (e.g., in a probably approximately correct sense [16]) by assuming that a large enough training set satisfying some statistical assumptions (e.g., independent and identically distributed examples) is available. However, it is difficult to obtain tight EGE bounds for DNNs due to the high-dimensional input and parameter settings DNNs are used in (e.g., thousands of inputs, such as pixels in an image, and millions of parameters) [37]. Thus, it remains a challenge to bound the classification error of DNNs used in real-world applications; in fact, several robustness issues with DNNs have been discovered (e.g., adversarial examples [28]).

As an alternative way of assuring the safety of systems using DNNs, researchers have focused on analyzing the *trained DNNs* used in specific systems [6–8, 15, 25, 32, 35, 36]. While analytic proofs of input/output properties are hard to obtain due to the complexity of DNNs (namely, they are universal function approximators [13]), prior work has shown it is possible to formally verify properties about DNNs by adapting existing satisfiability modulo theory (SMT) solvers [8, 15] and mixed-integer linear program (MILP) optimizers [7]. In particular, these techniques can verify linear properties about the DNN's output given linear constraints on the inputs. These approaches exploit the piecewise-linear nature of the rectified linear units (ReLUs) used in many DNNs and scale well by encoding the DNN as an input to efficient SMT/MILP solvers. As a result, existing tools can be used on reasonably sized DNNs, i.e., DNNs with several layers and a few hundred neurons per layer.

Although the SMT- and MILP-based approaches work well for the verification of properties of the DNN itself, these techniques cannot be straightforwardly extended to closed-loop systems using DNNs as controllers. Specifically, the non-linear dynamics of a typical CPS plant cannot be captured by these frameworks except for special cases such as discrete-time linear systems. While it is in theory possible to also approximate the plant dynamics with a ReLU-based DNN and verify properties about it, it is not clear how to relate properties of the approximating system to properties of the actual plant. As a result, it is challenging to use existing techniques to reason about the safety of the overall system.

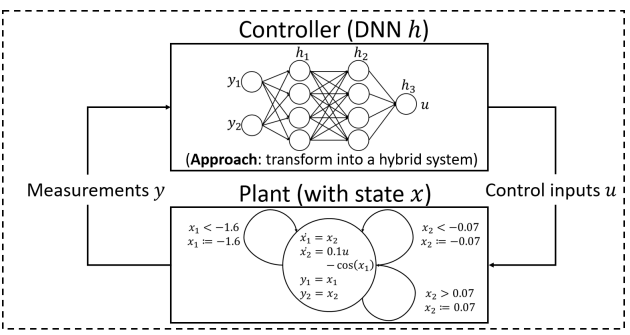
To overcome this limitation, we investigate an alternative approach, named Verisig, that allows us to verify properties of the closed-loop system. In particular, we consider CPS using sigmoid-based DNNs instead of ReLU-based ones and use the fact that the sigmoid is the solution to a quadratic differential equation. This allows us to transform the DNN into an equivalent hybrid system such that a DNN with L layers and N neurons per layer can be represented as a hybrid system with L+1 modes and 2N states. In turn, we compose the DNN's hybrid system with the plant's and verify properties of the composed system's reachable space by using existing reachability tools such as dReach [17] and Flow* [4].

To analyze the feasibility of the proposed approach, we show that the DNN reachability problem (i.e., checking whether the DNN's outputs lie in some set given constraints on the inputs) can be transformed into a real-arithmetic property with transcendental functions, which is decidable if Schanuel's conjecture is true [34]. We also prove that reachability is decidable for DNNs with one hidden layer, given interval constraints on the inputs. Finally, by casting the problem in the dReach framework, we also show that reachability is δ -decidable for general DNNs [10].

To evaluate the applicability of Verisig, we consider two case studies, one from reinforcement learning (RL) and one where a DNN is used to approximate an MPC with safety guarantees. DNNs are increasingly being used in these domains, so it is essential to be able to verify properties of interest about such systems. We trained a DNN on a benchmark RL problem, Mountain Car (MC), and verified that the DNN achieves its control task (i.e., drive an underpowered car up a hill) within the problem constraints. In the MPC approximation setting, we used an existing technique to approximate an MPC with a DNN [26] and verified that a DNN-controlled quadrotor reaches its goal without colliding into obstacles.

Finally, we evaluate Verisig's scalability, as used with Flow*, by training DNNs of increasing size on the MC problem. For each DNN, we record the time it takes to compute the output's reachable set. For comparison, we implemented a piecewise-linear approach to approximate each sigmoid as suggested in prior work [7]; in this setting, the problem is cast as an MILP that can be solved by an optimizer such as Gurobi [24]. We observe that, at similar levels of approximation, the MILP-based approach is faster than Verisig+Flow* for small DNNs and DNNs with few layers. However, the MILP-based approach's runtimes increase exponentially for deeper networks whereas Verisig+Flow* scales linearly with the number of layers since the same computation is run for each layer. This is another positive feature of our technique since deeper networks are known to learn more efficiently than shallow ones [31].

In summary, this paper has three contributions: 1) we develop an approach to transform a DNN into a hybrid system, which allows us to cast the closed-loop system verification problem into a hybrid system verification problem; 2) we show that the DNN reachability problem is decidable for DNNs with one hidden layer and decidable for general DNNs if Schanuel's conjecture holds; 3) we evaluate both the applicability and scalability of Verisig using two case studies.



Problem: verify property ϕ about the closed-loop system

Figure 1: Illustration of the closed-loop system considered in this paper. The plant model is given as a standard hybrid system, whereas the controller is a DNN. The problem is to verify a property of the closed-loop system.

The rest of this paper is organized as follows. Section 2 states the problem addressed in this work. Section 3 analyzes the decidability of the verification problem, and Section 4 describes Verisig. Sections 5 and 6 present the case study evaluations in terms of applicability and scalability. Section 7 provides concluding remarks.

2 PROBLEM FORMULATION

This section formulates the problem considered in this paper. We consider a closed-loop system, as shown in Figure 1, with states x, measurements y, and a controller h. The states and measurements are formalized in the next subsection, followed by the (DNN) controller description and the problem statement itself.

2.1 Plant Model

We assume the plant dynamics are given as a hybrid system. A hybrid system's state space consists of a finite set of discrete modes and a finite number of continuous variables [18]. Within each mode, continuous variables evolve according to differential equations with respect to time. Furthermore, each mode contains a set of invariants that hold true while the system is in that mode. Transitions between modes are controlled by guards, i.e., conditions on the continuous variables. Finally, continuous variables can be reset during each mode transition. The formal definition is provided below.

DEFINITION 1 (HYBRID SYSTEM). A hybrid system with inputs u and outputs y is a tuple $H = (X, X_0, F, E, I, G, R, g)$ where

- $X = X_D \times X_C$ is the state space with $X_D = \{q_1, \dots, q_m\}$ and X_C a manifold;
- $X_0 \subseteq X$ is the set of initial states;
- $F: X \longrightarrow TX_C$ assigns to each discrete mode $q \in X_D$ a vector field f_q , i.e., $\dot{x}_c = f_q(x_c, u)$ in mode q;
- $E \subseteq X_D \times X_D$ is the set of mode transitions;
- $I: X_D \longrightarrow 2^{X_C}$ assigns to $q \in X_D$ an invariant of the form $I(q) \subseteq X_C$;
- $G: E \longrightarrow 2^{X_C}$ assigns to each edge $e = (q_1, q_2)$ a guard $U \subseteq I(q_1)$;
- $R: E \longrightarrow (2^{X_C} \longrightarrow 2^{X_C})$ assigns to each edge $e = (q_1, q_2)$ a reset $V \subseteq I(q_2)$;
- $g: X \longrightarrow \mathbb{R}^p$ is the observation model such that y = g(x).

2.2 DNN Controller Model

A DNN controller maps measurements y to control inputs u and can be defined as a function h as follows: $h: \mathbb{R}^p \to \mathbb{R}^q$. To simplify the presentation, we assume the DNN is a fully connected feedforward neural network. However, the proposed technique applies to all common classes such as convolutional, residual or recurrent DNNs. As illustrated in Figure 1, a typical DNN has a layered architecture and can be represented as a composition of its L layers:

$$h(y) = h_L \circ h_{L-1} \circ \cdots \circ h_1(y),$$

where each hidden layer h_i , $i \in \{1, ..., L-1\}$, has an element-wise (with each element called a neuron) non-linear activation function:

$$h_i(y) = a(W_i y + b_i).$$

Each h_i is parameterized by a weight matrix W_i and an offset vector b_i . The most common types of activation functions are

- ReLU: $a(y) := ReLU(y) = \max\{0, y\},\$
- sigmoid: $a(y) := \sigma(y) = 1/(1 + e^{-y}),$
- hyperbolic tangent: $a(y) := \tanh(y) = (e^y e^{-y})/(e^y + e^{-y})$.

As argued in the introduction, and different from most existing works that assume ReLU activation functions, this work considers sigmoid and tanh activation functions (which also fall in the broad class of sigmoidal functions). Finally, the last layer h_L is linear:¹

$$h_L(y) = W_L y + b_L,$$

which is parameterized by a matrix W_L and a vector b_L .

During training, the parameters $(W_1, b_1, \ldots, W_L, b_L)$ are learned through an optimization algorithm (e.g., stochastic gradient descent [11]) used on a training set. In this paper, we assume the DNN is already trained, i.e., all parameters are known and fixed.

2.3 Problem Statement

Given the plant model and the DNN controller model described in this section, we identify two verification problems. The first one is the reachability problem for the DNN itself.

PROBLEM 1. Let h be a DNN as described in Section 2.2. The DNN verification problem, expressed as property ϕ_{dnn} , is to verify a property ψ_{dnn} on the DNN's outputs u given constraints ξ_{dnn} on the inputs y:

$$\phi_{dnn}(y, u) \equiv (\xi_{dnn}(y) \land h(y) = u) \Rightarrow \psi_{dnn}(u). \tag{1}$$

Problem 2 is to verify a property of the closed-loop system.

PROBLEM 2. Let $S = h \mid\mid H_P$ be the composition of a DNN controller h (Section 2.2) and a plant P, modeled with a hybrid system H_P (Section 2.1). Given a property ξ on the initial states X_0 of P, the problem, expressed as property ϕ , is to verify a property ψ of the reachable states of P:

$$\phi(X_0, x(t)) \equiv \xi(X_0) \Rightarrow \psi(x(t)), \ \forall t \ge 0.$$
 (2)

Our approach to Problem 1, namely transforming the DNN into an equivalent hybrid system, also presents a solution to Problem 2 since we can compose the DNN's hybrid system with the plant's and can use existing hybrid system verification tools. APPROACH. We approach Problem 1 by transforming h into a hybrid system H_h such that if x_0 is an initial condition of H_h , then the only reachable state in the last mode of H_h is $h(x_0)$. Problem 2 is addressed by verifying safety for the composed hybrid system $H_h \parallel H_P$.

3 ON THE DECIDABILITY OF SIGMOID-BASED DNN REACHABILITY

Before describing our approach to the problems stated in Section 2, a natural question to ask is whether these problems are decidable. The answer is not obvious due to the non-linear nature of the sigmoid. This section shows that if the DNN's inputs and outputs are given as a real-arithmetic property, then reachability can be stated as a real-arithmetic property with transcendental functions, which is decidable if Schanuel's conjecture is true [34]. Furthermore, we prove decidability for the case of NNs with a single hidden layer, under mild assumptions on the DNN parameters. Finally, we argue that by casting the DNN verification problem into a hybrid system verification problem, we obtain a δ -decidable problem [10].²

3.1 DNNs with multiple hidden layers

As formalized in Section 2, the reachability property of a DNN h with inputs y and outputs y has the general form:

$$\phi(y, u) \equiv (\xi(y) \land h(y) = u) \Rightarrow \psi(u), \tag{3}$$

where ξ and ψ are given properties on the real numbers. Verifying properties on the real numbers is undecidable in general. A notable exception is first-order logic formulas over $(\mathbb{R}, <, +, -, \cdot, 0, 1)$, i.e., the language where < is the relation, +, -, and \cdot are functions, and 0 and 1 are the constants [30]; we denote such formulas by \mathcal{R} -formulas. Intuitively, \mathcal{R} -formulas are first-order logic statements where the constraints are polynomial functions of the variables with integer coefficients. Example \mathcal{R} -formulas are $\forall x \ \forall y : xy > 0, \exists x : x^2 - 2 = 0$, and $\exists w : xw^2 + yw + z = 0$.

Another relevant language is (\mathbb{R} , <, +, -, ·, exp, 0, 1), which also includes exponentiation; we denote these formulas by \mathcal{R}_{exp} -formulas. Although it is an open question whether verifying \mathcal{R}_{exp} -formulas is decidable, it is known that decidability is connected to Schanuel's conjecture [34]. Schanuel's conjecture concerns the transcendence degree of certain field extensions of the rational numbers and, if true, would imply that verifying \mathcal{R}_{exp} -formulas is decidable [34].

We focus on the case where ξ and ψ are \mathcal{R} -formulas. The exponentiation in the sigmoid means that ϕ , however, is not a \mathcal{R} -formula. We show below that ϕ is in fact an \mathcal{R}_{\exp} -formula, which implies that DNN reachability is decidable if Schanuel's conjecture is true [34].

PROPOSITION 3.1. Let $h: \mathbb{R}^p \to \mathbb{R}^q$ be a sigmoid-based DNN with L-1 hidden layers (with N neurons each) and rational parameters. The property $\phi(y,u) \equiv (\xi(y) \land h(y) = u) \Rightarrow \psi(u)$, where ξ and ψ are \mathcal{R} -formulas, is an \mathcal{R}_{exp} -formula.

 $^{^1}$ The last layer is by convention a linear layer, although it could also have a non-linear activation, as shown in the Mountain Car case study.

 $^{^2\}mathrm{Note}$ that the results presented in this section hold for DNNs with sigmoid activation functions, but similar results can be shown for tanh.

PROOF. Since ψ is an \mathcal{R} -formula, it suffices to show that $\phi_0(y, u) \equiv \xi(y) \wedge h(y) = u$ can be expressed as an \mathcal{R}_{\exp} -formula. Note that

$$\begin{split} \phi_0(y,u) &\equiv \xi(y) \wedge h_1^1 = \frac{1}{1 + \exp\{-(w_1^1)^\top y - b_1^1\}} \wedge \dots \\ &\wedge h_1^N = \frac{1}{1 + \exp\{-(w_1^N)^\top y - b_1^N\}} \wedge \dots \\ &\wedge h_{L-1}^1 = \frac{1}{1 + \exp\{-(w_{L-1}^1)^\top h_{L-2} - b_{L-1}^1\}} \wedge \dots \\ &\wedge h_{L-1}^N = \frac{1}{1 + \exp\{-(w_{L-1}^1)^\top h_{L-2} - b_{L-1}^N\}} \\ &\wedge u &= W_L [h_{L-1}^1, \dots, h_{L-1}^N]^\top + b_L, \end{split}$$

where $(w_i^j)^{\top}$ is row j of W_i , and $h_l = [h_l^1, \dots, h_l^N]^{\top}, l \in \{1, \dots, L-1\}$. The last constraint, call it p(u), is already an \mathcal{R} -formula. Let $[W_i]_{jk} = p_{jk}^i/q_{jk}^i$, with p_{jk}^i and $q_{jk}^i > 0$ integers, and let $d_0 = q_{11}^1q_{12}^1\cdots q_{Np}^{L-1}$. To remove fractions from the exponents, we add extra variables z_i and v_i^j and arrive at an equivalent property $\phi_{\mathbb{Z}}$, which is an \mathcal{R}_{exp} -formula since all denominators are \mathcal{R}_{exp} -formulas:

$$\begin{split} \phi_{\mathbb{Z}}(y,u) &\equiv \ \xi(y) \wedge z_0 d_0 = y \wedge h_1^1 = \frac{1}{1 + \exp\{-(r_1^1)^\top z_0 - v_1^1\}} \wedge \dots \\ \wedge \ h_1^N &= \frac{1}{1 + \exp\{-(r_1^N)^\top z_0 - v_1^N\}} \wedge v_1^1 = b_1^1 \wedge \dots \wedge v_1^N = b_1^N \wedge \dots \\ \wedge \ z_{L-2} d_0 &= h_{L-2} \wedge h_{L-1}^1 = \frac{1}{1 + \exp\{-(r_{L-1}^1)^\top z_{L-2} - v_{L-1}^1\}} \wedge \dots \\ \wedge \ h_{L-1}^N &= \frac{1}{1 + \exp\{-(r_{L-1}^N)^\top z_{L-2} - v_{L-1}^N\}} \\ \wedge \ v_{L-1}^1 &= b_{L-1}^1 \wedge \dots \wedge v_{L-1}^N = b_{L-1}^N \wedge p(u), \end{split}$$

where $r_i^j = w_i^j d_0$ are vectors of integers; $v_i^j = b_i^j$ are \mathcal{R} -formulas since b_i^j are rational.

COROLLARY 3.2 ([34]). If Schanuel's conjecture holds, then verifying the property $\phi(y,u) \equiv (\xi(y) \land h(y) = u) \Rightarrow \psi(u)$ is decidable under the conditions stated in Proposition 3.1.

Remark. Note that by transforming the DNN into an equivalent hybrid system (as described in Section 4), we show that DNN reachability is δ -decidable as well [10]. Intuitively, δ -decidability means that relaxing all constraints by a rational δ results in a decidable problem; as shown in prior work [10], reachability is δ -decidable for hybrid systems with dynamics given by Type 2 computable functions, which is large class of functions that contains the sigmoid.

3.2 Neural Networks with a single hidden layer

Regardless of whether Schanuel's conjecture holds, we can show that DNN reachability is decidable for networks with a single hidden layer. In particular, assuming interval bounds are given for each input, it is possible to transform the reachability property into an \mathcal{R} -formula, thus showing that verifying reachability is decidable.

Theorem 3.3. Let $h: \mathbb{R}^p \to \mathbb{R}^q$ be a sigmoid-based neural network with rational parameters and with one hidden layer (with N

neurons), i.e., $h(x) = W_2(\sigma(W_1x + b_1)) + b_2$. Let $[W_1]_{ij} = p_{ij}/q_{ij}$ and let $d_0 = q_{11}q_{12} \cdots q_{Np}$. Consider the property

$$\phi(y, u) \equiv \exists y \ (y \in I_y \land u = h(y)) \Rightarrow \psi(u),$$

where $y = [y_1, \ldots, y_p]^{\top} \in \mathbb{R}^p$, $u = [u_1, \ldots, u_q]^{\top} \in \mathbb{R}^q$, ψ is an \mathcal{R} -formula, and $I_y = [\alpha_1, \beta_1] \times \cdots \times [\alpha_p, \beta_q] \subseteq \mathbb{R}^p$, i.e., the Cartesian product of p one-dimensional intervals. Then verifying $\phi(y, u)$ is decidable if, for all $i \in \{1, \ldots, N\}$ and $j \in \{1, \ldots, p\}$, $e^{b_1^i}$, e^{α_j/d_0} , and e^{β_j/d_0} are rational, i.e., $b_1^i = \ln(b_r^i)$, $\alpha_j = d_0 \ln(\alpha_r^j)$ and $\beta_j = d_0 \ln(\beta_r^j)$ for some rational numbers b_r^i , α_r^j , and β_r^j .

PROOF. The proof technique borrows ideas from [18]. It suffices to show that $\phi(y, u)$ is an \mathcal{R} -formula. Since $\psi(u)$ is an \mathcal{R} -formula, we focus on the left-hand side of the implication, call it $\phi_0(y, u)$:

$$\phi_0(y, u) \equiv y \in I_y \wedge h_1^1 = \frac{1}{1 + \exp\{-(w_1^1)^\top y - b_1^1\}} \wedge \dots$$
$$\wedge h_1^N = \frac{1}{1 + \exp\{-(w_1^N)^\top y - b_1^N\}} \wedge u = W_2[h_1^1, \dots, h_1^N]^\top + b_2,$$

where $(w_1^i)^{\top}$ is row i of W_1 . Note that the last constraint in $\phi_0(y, u)$, call it p(u), is an \mathcal{R} -formula. To remove fractions from the exponentials, we change the limits of y. Consider the property

$$\phi_{\mathbb{Z}}(y,u) \equiv y \in I_{y}^{\mathbb{Z}} \wedge h_{1}^{1} = \frac{1}{1 + \exp\{-(r_{1}^{1})^{\top}y - b_{1}^{1}\}} \wedge \dots$$
$$\wedge h_{1}^{N} = \frac{1}{1 + \exp\{-(r_{1}^{N})^{\top}y - b_{1}^{N}\}} \wedge p(u),$$

where $I_y^{\mathbb{Z}} = [\alpha_1/d_0, \beta_1/d_0] \times \cdots \times [\alpha_p/d_0, \beta_p/d_0]$ and each $r_1^i = d_0 w_1^i$ is a vector of integers. Note that $\phi_0(y, u) \equiv \phi_{\mathbb{Z}}(y, u)$, since a change of variables $z = y/d_0$ implies that $z \in I_y^{\mathbb{Z}}$ iff $y \in I_y$. To remove exponentials from the constraints, we use their monotonicity property and transform $\phi_{\mathbb{Z}}(x, y)$ into an equivalent property $\phi_e(x, y)$:

$$\phi_{e}(y,u) \equiv y \in I_{y}^{e} \wedge h_{1}^{1} = \frac{1}{1 + y_{1}^{r_{11}^{1}} \cdots y_{p}^{r_{1p}^{1}} \exp\{-b_{1}^{1}\}} \wedge \dots$$

$$\wedge h_{1}^{N} = \frac{1}{1 + y_{1}^{r_{11}^{N}} \cdots y_{p}^{r_{1p}^{N}} \exp\{-b_{1}^{N}\}} \wedge p(u),$$

where $I_y^e = [e^{-\beta_1/d_0}, e^{-\alpha_1/d_0}] \times \cdots \times [e^{-\beta_P/d_0}, e^{-\alpha_P/d_0}]$, and r_{1j}^i is element j of r_1^i . To see that $\phi_e(y,u) \equiv \phi_{\mathbb{Z}}(y,u)$, take any $y \in I_y^{\mathbb{Z}}$ and note that $\exp\{-r_{1j}^iy_j\} = z_j^{r_{1j}^i}$, with $z_j = e^{-y_j}$; thus, $z \in I_x^e$. The final step transforms the property $\phi_e(y,u)$ into an equivalent

The final step transforms the property $\phi_e(y, u)$ into an equivalent property v(y, u) to eliminate negative integers r_{1i}^i in the exponents:

$$\begin{split} v(y,u) &\equiv y \in I_y^e \; \exists z \in I_y^{e^-} \; y_1 z_1 = 1 \wedge \dots \wedge y_p z_p = 1 \\ &\wedge h_1^1 = \frac{1}{1 + \prod_{j \in I_1^+} y_j^{r_{1j}^1} \prod_{j \in I_1^-} z_j^{-r_{1j}^1} \exp\{-b_1^1\}} \wedge \dots \\ &\wedge h_1^N = \frac{1}{1 + \prod_{j \in I_1^+} y_{jj}^{r_{1j}^N} \prod_{j \in I_{3j}^-} z_j^{-r_{1j}^N} \exp\{-b_1^N\}} \wedge p(u), \end{split}$$

Verisig: verifying hybrid systems with neural network controllers

where $I_y^{e^-} = [e^{\alpha_1/d_0}, e^{\beta_1/d_0}] \times \cdots \times [e^{\alpha_p/d_0}, e^{\beta_p/d_0}], I_i^+ = \{k \mid r_{1k}^i \geq 0\}, \text{ and } I_i^- = \{k \mid r_{1k}^i < 0\}. \text{ Note that } \phi_e(y, u) \equiv v(y, u) \text{ since for } r_{1j}^i < 0, \text{ the constraint } z_j y_j = 1 \text{ implies } y_j^{r_{1j}^i} = z_j^{-r_{1j}^i}.$

Thus, if $e^{b_1^j}$, e^{α_i/d_0} , and e^{β_i/d_0} are rational for all $i \in \{1, \ldots, p\}$, $j \in \{1, \ldots, N\}$, one can show that v(y, u) is an \mathcal{R} -formula by multiplying all h_1^i constraints by their denominators. All denominators are positive since y_i and z_i are constrained to be positive.

The single-layer assumption in Theorem 3.3 is not too restrictive since DNNs with one hidden layer are still universal approximators. At the same time, the technique used to prove Theorem 3.3 cannot be applied to multiple hidden layers since the DNN becomes an \mathcal{R}_{exp} -formula in that case. Note that it might be possible to show more general versions of Theorem 3.3 by relaxing the interval constraints or the real-arithmetic constraints. Finally, note that the assumption on the DNN's weights is mild since a DNN's weights can be altered in such a way that they are arbitrarily close to the original weights while also satisfying the theorem's requirements.

4 DNN REACHABILITY USING HYBRID SYSTEMS

Having analyzed the decidability of DNN reachability in Section 3, in this section we investigate an approach to computing the DNN's reachable set. In particular, we transform the DNN into an equivalent hybrid system, which allows us to use existing hybrid system reachability tools such as Flow*. Sections 4.1 and 4.2 explain the transformation technique, and Section 4.3 provides an illustrative example. Finally, Section 4.4 discusses existing hybrid system reachability tools. Note that this section focuses on the case of sigmoid activations; the treatment of tanh activations is almost identical—the differences are noted in the relevant places in the section.

4.1 Sigmoids as solutions to differential equations

The main observation that allows us to transform a DNN into an equivalent hybrid system is the fact that the sigmoid derivative can be expressed in terms of the sigmoid itself:³

$$\frac{d\sigma}{dx}(x) = \sigma(x)(1 - \sigma(x)). \tag{4}$$

Thus, the sigmoid can be treated as a quadratic dynamical system. Since we would like to know the possible values of the sigmoid for a given set of inputs, we introduce a "time" variable t that is multiplied by the inputs. In particular, consider the proxy function

$$g(t,x) = \sigma(tx) = \frac{1}{1 + e^{-xt}},$$
 (5)

such that $g(1, x) = \sigma(x)$ and, by the chain rule,

$$\frac{\partial g}{\partial t}(t,x) = \dot{g}(t,x) = xg(t,x)(1 - g(t,x)). \tag{6}$$

Thus, by tracing the dynamics of g until time t=1, we obtain exactly the value of $\sigma(x)$; the initial condition is g(0,x)=0.5, as can be verified from (5). While the intermediate values of the sigmoid states are not considered, the integration allows us to iteratively construct the sigmoid's reachable set. To avoid the integration, one

needs to find a computationally cheap, yet expressive, representation of this reachable set. We leave investigating this approach for future work. Since each neuron in a sigmoid-based DNN is a sigmoid function, we can use the proxy function \boldsymbol{g} to transform the entire DNN into a hybrid system, as described next.

4.2 Deep Neural Networks as Hybrid Systems

Given the proxy function g described in Section 4.1, we now show how to transform a DNN into a hybrid system. Let N_i be the number of neurons in hidden layer h_i and let h_{ij} denote neuron j in h_i , i.e.,

$$h_{ij}(x) = \sigma((w_i^j)^\top x + b_i^j), \tag{7}$$

where $(w_i^j)^{\top}$ is row j of W_i and b_i^j is element j of b_i . Given h_{ij} , the corresponding proxy function g_{ij} is defined as follows:

$$g_{ij}(t,x) = \sigma(t \cdot ((w_i^j)^\top x + b_i^j)) = \frac{1}{1 + \exp\{-t \cdot ((w_i^j)^\top x + b_i^j)\}},$$

where, once again, $g_{ij}(1, x) = h_{ij}(x)$. Note that, by the chain rule,

$$\frac{\partial g_{ij}}{\partial t}(t,x) = \dot{g}_{ij}(t,x) = ((w_i^j)^\top x + b_i^j)g_{ij}(t,x)(1 - g_{ij}(t,x)).$$
 (8)

Thus, for a given x, the value of hidden layer $h_i(x)$ can be obtained by tracing all $g_{ij}(t,x)$ until t=1 (initialized at $g_{ij}(0,x)=0.5$). This suggests that each hidden layer can be represented as a set of differential equations $g_{ij}(t,x)$, where g_{ij} can be considered a state.

With the above intuition in mind, we now show how to transform the DNN into an equivalent hybrid system. To simplify notation, we assume $N=N_i$ for all $i\in\{1,\ldots,L-1\}$; we also assume the DNN has only one output. The proposed approach can be extended to the more general case by adding more states in the hybrid system.

The hybrid system has one mode for each DNN layer. To ensure the hybrid system is equivalent to the DNN, in each mode we trace $g_{ij}(t,x)$ until t=1 by using the differential equations $\dot{g}_{ij}(t,x)$ in (8). Thus, we use N continuous states, x_1^P,\ldots,x_N^P , to represent the proxy variables for each layer; when in mode i, each $x_j^P, j \in \{1,\ldots,N\}$, represents neuron h_{ij} in the DNN. We also introduce N additional continuous states (one per neuron), x_1^J,\ldots,x_N^J , to keep track of the linear functions within each neuron. The x_i^J states are necessary because the inputs to each neuron are functions of the x_i^P states reached in the previous mode.

The hybrid system description is formalized in Proposition 4.1. The extra mode q_0 is used to reset the x_i^P states to 0.5 and the x_i^J states to their corresponding values in q_1 . The two extra states, t and u, are used to store the "time" and the DNN's output, respectively. Note that \odot denotes Hadamard (element-wise) product.

PROPOSITION 4.1. Let $h: \mathbb{R}^p \to \mathbb{R}^1$ be a sigmoid-based DNN with L-1 hidden layers (with N neurons each) and a linear last layer with one output. The image under h of a given set I_y is exactly the reachable set for u in mode q_L of the following hybrid system:

- Continuous states: $x^P = [x_1^P, \dots, x_N^P]^\top, x^J = [x_1^J, \dots, x_N^J]^\top, u.t$:
- Discrete states (modes): q_0, q_1, \ldots, q_L ;
- Initial states: $x^P \in I_y$, $x^J = 0$, u = 0, t = 0;
- Flow

$$-F(q_0) = [\dot{x}^P = 0, \dot{x}^J = 0, \dot{u} = 0, \dot{t} = 1];$$

³The corresponding differential equation for tanh is $(d\tanh/dx)(x) = 1 - \tanh^2(x)$.

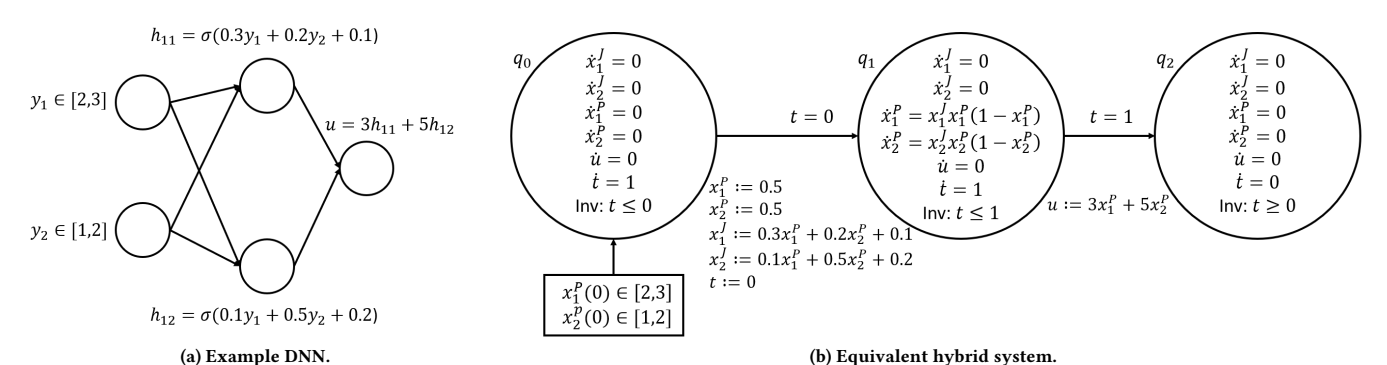


Figure 2: Small example illustrating the transformation from a DNN to a hybrid system.

```
\begin{split} &-F(q_i) = [\dot{x}^P = x^J \odot x^P \odot (1-x^P), \dot{x}^J = 0, \dot{u} = 0, \dot{t} = 1] \\ & for \ i \in \{1, \dots, L-1\}; \\ &-F(q_L) = [\dot{x}^P = 0, \dot{x}^J = 0, \dot{u} = 0, \dot{t} = 0]; \\ &\bullet Transitions: E = \{(q_0, q_1), \dots, (q_{L-1}, q_L)\}; \\ &\bullet Invariants: \\ &-I(q_0) = \{t \leq 0\}; \\ &-I(q_i) = \{t \leq 1\} \ for \ i \in \{1, \dots, L-1\}; \\ &-I(q_L) = \{t \leq 0\}; \\ &\bullet Guards: \\ &-G(q_0, q_1) = \{t = 0\}; \\ &-G(q_0, q_{1+1}) = \{t = 1\} \ for \ i \in \{1, \dots, L-1\}; \\ &\bullet Resets: \\ &-R(q_i, q_{i+1}) = \{x^P = 0.5, x^J = W_i x^P + b_i, t = 0\} \\ &for \ i \in \{0, \dots, L-2\}; \\ &-R(q_{L-1}, q_L) = \{u = W_L x^P + b_L\}. \end{split}
```

PROOF. First note that the reachable set of x^P in mode q_1 at time t=1 is exactly the image of I_y under h_1 , the first hidden layer. This is true because at t=1, x^P takes the value of the sigmoid function. Applying this argument inductively, the reachable set of x^P in mode q_{L-1} at time t=1 is exactly the image of I_y under $h_{L-1} \circ \cdots \circ h_1$. Finally, u is a linear function of x^P with the same parameters as the last linear layer of h. Thus, the reachable set for u in mode q_L is the image of I_y under $h_L \circ \cdots \circ h_1 = h$.

We emphasize that the "time" in the sigmoid dynamics is local to the DNN. When the DNN's hybrid system is composed with the plant's, a separate time variable will be used to store global time (which is paused during the sigmoid computation). This captures all common CPS where the controller is either time- or event-triggered.

4.3 Illustrative Example

To illustrate the transformation process from a DNN to a hybrid system, this subsection presents a small example, shown in Figure 2. The two-layer DNN is transformed into an equivalent three-mode hybrid system. Since all the weights are positive and the sigmoids are monotonically increasing, the maximum value for the DNN's output u is achieved at the maximum values of the inputs, whereas the minimum value for u is achieved at the minimum values of the inputs, i.e., $u \geq 3\sigma(0.3 \cdot 2 + 0.2 \cdot 1 + 0.1) + 5\sigma(0.1 \cdot 2 + 0.5 \cdot 1 + 0.2)$ and $u \leq 3\sigma(0.3 \cdot 3 + 0.2 \cdot 2 + 0.1) + 5\sigma(0.1 \cdot 3 + 0.5 \cdot 2 + 0.2)$. The same conclusion can be reached about state u in the hybrid system.

4.4 Hybrid System Verification Tools

Depending on the hybrid system model and the desired precision, there are multiple tools one might use. In the case of linear hybrid systems, there are powerful tools that scale up to a few thousand states [9]. For non-linear systems, reachability is undecidable in general, except for specific subclasses [2, 18]. Despite this negative result, multiple reachability methods have been developed that have proven useful in specific scenarios. In particular, Flow* [4] works by constructing flowpipe overapproximations of the dynamics in each mode using Taylor Models; although Flow* provides no decidability claims, it scales well in practice. Alternatively, dReach [17] provides δ -decidability guarantees for Type 2 computable functions; at the same time, dReach is not as scalable and could not handle more than a few dozen variables in the examples tried in this paper. Finally, one can also use SMT solvers such as z3 [22]; yet, SMT solvers are not optimized for non-linear arithmetic and do not scale well either.

In this paper, we use Flow* due to its scalability; as shown in the evaluation, it efficiently handles systems with a few hundred states, i.e., DNNs with a few hundred neurons per layer. Furthermore, the mildly non-linear nature of the sigmoid dynamics suggests that the approximations used in Flow* are sufficiently precise so as to verify interesting properties. This is illustrated in the case studies as well as in the scalability evaluation in Section 6.

Finally, note that all existing tools have been developed for large classes of hybrid systems and do not exploit the specific properties of the sigmoid dynamics, e.g., they are monotonic and polynomial. For example, in some cases it is possible to symbolically compute the reachable set of monotone systems [5], although directly applying this approach to our setting does not work due to the large state space. Thus, developing a specialized sigmoid reachability tool is bound to greatly improve scalability and precision; since this paper is a proof of concept, developing such a tool is left for future work.

5 CASE STUDY APPLICATIONS

This section presents two case studies in order to illustrate possible use cases for the proposed verification approach. These case studies were chosen in domains where DNNs are used extensively as controllers, with weak worst-case guarantees about the trained network. This means it is essential to verify properties about these closed-loop systems in order to assure their functionality. The first case study, presented in Section 5.1, is Mountain Car, a benchmark



Figure 3: Mountain Car problem [23]. The car needs to drive up the left hill first in order to gather enough momentum.

problem in RL. Section 5.2 presents the second case study in which a DNN is used to approximate an MPC with safety guarantees.

5.1 A Reinforcement Learning Case Study

This subsection illustrates how Verisig could be used on a benchmark RL problem, namely Mountain Car (MC). In MC, an underpowered car must drive up a steep hill, as shown in Figure 3. Since the car does not have enough power to accelerate up the hill, it needs to drive up the opposite hill first in order to gather enough momentum. The learning task is to learn a controller that takes as input the car's position and velocity and outputs an acceleration command. The car has the following discrete-time dynamics:

$$p_{k+1} = p_k + v_k$$

$$v_{k+1} = v_k + 0.0015u_k - 0.0025 * cos(3p_k),$$

where u_k is the controller's input, and p_k and v_k are the car's position and velocity, respectively, with p_0 chosen uniformly at random from [-0.6, -0.4] and $v_0 = 0$. Note that v_k is constrained to be within [-0.07, 0.07] and p_k is constrained to be within [-1.2, 0.6], thereby introducing (hybrid) mode switches when these constraints are violated. We consider the continuous version of the problem such that u_k is a real number between -1 and 1.

During training, the learning algorithm tries different control actions and observes a reward. The reward associated with a control action u_k is $-0.1u_k^2$, i.e., larger control inputs are penalized more so as to avoid a "bang-bang" strategy. A reward of 100 is received when the car reaches its goal. The goal of the training algorithm is to maximize the car's reward. The training stage typically occurs over multiple episodes (if not solved, an episode is terminated after 1000 steps) such that various behaviors can be observed. MC is considered "solved" if, during testing, the car goes up the hill with an average reward of at least 90 over 100 consecutive trials.

Using Verisig, one can strengthen the definition of a "solved" task and *verify* that the car will go up the hill with a reward of at least 90 starting from *any* initial condition. To illustrate this, we trained a DNN controller for MC in OpenAI Gym [23], a toolkit for developing and comparing algorithms on benchmark RL problems. We utilized a standard actor/critic approach for deep RL problems [19]. This is a two-DNN setting in which one DNN (the critic) learns the reward function, whereas the other one (the actor) learns the control. Once training is finished, the actor is deployed as the DNN controller for the closed-loop system. We trained a two-hidden-layer sigmoid-based DNN with 16 neurons per layer; the last layer

| Initial condition | Verified | Reward | # steps | Time |
|-------------------|----------|--------|---------|-------|
| [-0.41, -0.40] | Yes | >= 90 | <= 100 | 1336s |
| [-0.415, -0.41] | Yes | >= 90 | <= 100 | 1424s |
| [-0.42, -0.415] | Yes | >= 90 | <= 100 | 812s |
| [-0.43, -0.42] | Yes | >= 90 | <= 100 | 852s |
| [-0.45, -0.43] | Yes | >= 90 | <= 100 | 886s |
| [-0.48, -0.45] | Yes | >= 90 | <= 100 | 744s |
| [-0.50, -0.48] | Yes | >= 90 | <= 100 | 465s |
| [-0.53, -0.50] | Yes | >= 90 | <= 100 | 694s |
| [-0.55, -0.53] | Yes | >= 90 | <= 100 | 670s |
| [-0.57, -0.55] | Yes | >= 90 | <= 100 | 763s |
| [-0.58, -0.57] | Yes | >= 90 | <= 109 | 793s |
| [-0.59, -0.58] | Yes | >= 90 | <= 112 | 1307s |
| [-0.6, -0.59] | No | N/A | N/A | N/A |

Table 1: Verisig+Flow* verification times (in seconds) for different initial conditions of MC. The third column shows the verified lower bound of reward. The fourth column shows the verified upper bound of the number of dynamics steps.

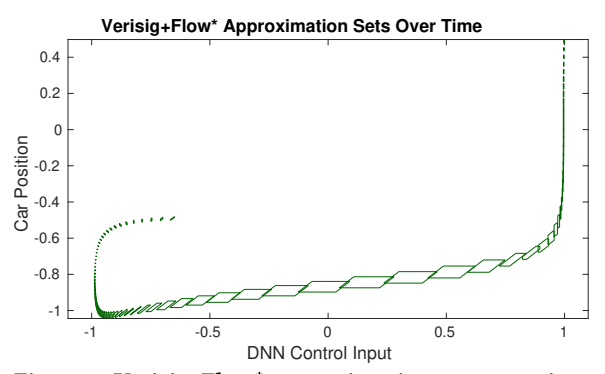


Figure 4: Verisig+Flow* approximation sets over time.

has a tanh activation function in order to scale the output to be between -1 and 1. Note that larger networks were also trained in order to evaluate scalability, as discussed in Section 6.

To verify that the car will go up the hill with a reward of at least 90, we transform the DNN into an equivalent hybrid system using Verisig and compose it with the car's hybrid system. We use Verisig+Flow* to verify the desired property on the composed system, given any initial position in [-0.6, -0.4]. Note that we split the initial condition into subsets and verify the property for each subset separately. This is necessary because the DNN takes very different actions from different initial conditions, e.g., large negative inputs when the car is started from the leftmost position and small negative inputs for larger initial conditions. This variability introduces uncertainty in the dynamics and causes large approximation errors. As part of future work, we will investigate a refinement procedure in order to optimize the partitioning of the initial condition.

Table 1 presents the verification times for each subset. Most properties are verified within 10-15 minutes; the properties at either end of the initial set take longer to verify due to branching in the car's hybrid system as caused by the car reaching the minimum allowed position. For most initial conditions, we verify that the car will go up the hill with a reward of at least 90 and in at most 100 dynamics steps. Interestingly, after failing to verify the property for

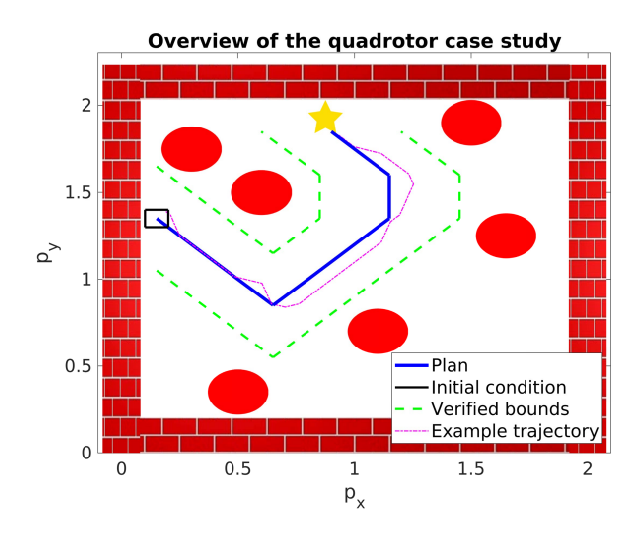


Figure 5: Overview of the quadrotor case study, as projected to the (p_x, p_y) -plane. The quadrotor follows its plan in order to reach the goal (star) without colliding into obstacles (red circles). We verify that, starting from any initial condition in the black box, the quadrotor does not deviate from its plan by more than 0.32m and does not collide into obstacles.

the subset [-0.6, -0.59], we found a counter-example when starting the car from $p_0 = -0.6$: the final reward was 88. This suggests that Verisig is not only useful for verifying properties of interest but it can also be used to identify areas for which these properties do not hold. In the case of MC, this information can be used to retrain the DNN by starting more episodes from [-0.6, -0.59] since the likely reason the DNN does not perform well from that initial set is that not many episodes were started from there during training.

Finally, we illustrate the progression of the approximation sets created by Flow*. Figure 4 shows a two-dimensional projection of the approximation sets over time (for the case $p_0 \in [-0.5, -0.48]$), with the DNN control inputs plotted on the x-axis and the car's position on the y-axis. Initially, the uncertainty is fairly small and remains so until the car goes up the left hill and starts going quickly downhill. At that point, the uncertainty increases but it remains within the tolerance necessary to verify the desired property.

5.2 Using DNNs to Approximate MPCs with Safety Guarantees

To further evaluate the applicability of Verisig, we also consider a case study in which a DNN is used to approximate an MPC with safety guarantees. DNNs are used to approximate controllers for several reasons: 1) the MPC computation is not feasible at runtime [12]; 2) storing the original controller (e.g., as a lookup table) requires too much memory [14]; 3) performing reachability analysis by discretizing the state space is infeasible for high-dimensional systems [26]. We focus on the latter scenario in which the aim is to develop a DNN controller with safety guarantees.

As described in prior work [26], it is possible to train a DNN to approximate an MPC in the case of control-affine systems whose goal is to follow a piecewise-linear plan. In this case, the optimal controller is "bang-bang", i.e., it is effectively a classifier mapping a

| Property | Time |
|-------------------------------|---|
| $ r_3 _{\infty} \le 0.32m$ | 2766s |
| $ r_3 _{\infty} \le 0.32m$ | 2136s |
| $ r_3 _{\infty} \le 0.32m$ | 2515s |
| $ r_3 _{\infty} \le 0.32m$ | 897s |
| $ r_3 _{\infty} \le 0.32m$ | 1837s |
| $ r_3 _{\infty} \le 0.32m$ | 1127s |
| $ r_3 _{\infty} \le 0.32m$ | 1593s |
| $ r_3 _{\infty} \le 0.32m$ | 894s |
| $ r_3 _{\infty} \le 0.32m$ | 1376s |
| $ r_3 _{\infty} \le 0.32m$ | 953s |
| $ r_3 _{\infty} \le 0.32m$ | 1038s |
| $ r_3 _{\infty} \leq 0.32m$ | 647s |
| $ r_3 _{\infty} \le 0.32m$ | 3534s |
| $ r_3 _{\infty} \le 0.32m$ | 2491s |
| $ r_3 _{\infty} \le 0.32m$ | 2142s |
| $ r_3 _{\infty} \leq 0.32m$ | 1090s |
| | $ r_3 _{\infty} \le 0.32m$ |

Table 2: Verisig+Flow* verification times (in seconds) for different initial conditions of the quadrotor case study. All properties were verified. Note that $r_3 = [p_x^r, p_y^r, p_z^r]$.

system state to one of finitely many control actions. Once the DNN is trained, it can be used on the system instead of the MPC. Although worst-case deviations from the planner can be obtained for specific initial points, it is not known whether the DNN controller is safe for a range of initial conditions. Thus, we use Verisig to verify the safety of such a closed-loop system.

In this case study, we consider a six-dimensional control-affine model for a quadrotor controlled by a DNN and verify that the quadrotor reaches its goal without colliding into nearby obstacles. Specifically, the quadrotor follows a planner, given as a piecewise-linear system, and tries to stay as close to the planner as possible. The setup, as projected to the (p_x,p_y) -plane, is shown in Figure 5. The quadrotor and planner dynamics models are as follows:

$$\dot{q} := \begin{bmatrix} \dot{p}_{x}^{q} \\ \dot{p}_{y}^{q} \\ \dot{p}_{y}^{q} \\ \dot{p}_{z}^{q} \\ \dot{v}_{y}^{q} \\ \dot{v}_{y}^{q} \\ \dot{v}_{z}^{q} \end{bmatrix} = \begin{bmatrix} v_{x}^{q} \\ v_{x}^{q} \\ v_{y}^{q} \\ v_{z}^{q} \\ g \tan \theta \\ -g \tan \phi \\ \tau - q \end{bmatrix}, \dot{p} := \begin{bmatrix} \dot{p}_{x}^{p} \\ \dot{p}_{y}^{p} \\ \dot{p}_{y}^{p} \\ \dot{v}_{x}^{p} \\ \dot{v}_{y}^{p} \\ \dot{z}^{p} \end{bmatrix} = \begin{bmatrix} b_{x} \\ b_{y} \\ b_{z} \\ 0 \\ 0 \\ 0 \end{bmatrix}, \quad (9)$$

where p_x^q, p_y^q, p_z^q and p_x^p, p_y^p, p_z^p are the quadrotor and planner's positions, respectively; v_x^q, v_y^q, v_z^q and v_x^p, v_y^p, v_z^p are the quadrotor and planner's velocities, respectively; θ, ϕ and τ are control inputs (for pitch, roll and thrust); $g = 9.81 m/s^2$ is gravity; b_x, b_y, b_z are piecewise constant functions of time. The control inputs have constraints $\phi, \theta \in [-0.1, 0.1]$ and $\tau \in [7.81, 11.81]$; the planner velocities have constraints $b_x, b_y, b_z \in [-0.25, 0.25]$. The controller's goal is to ensure the quadrotor is as close to the planner as possible, i.e., stabilize the system of relative states $r := [p_x^r, p_y^r, p_z^r, v_x^r, v_y^r, v_z^r]^\top = q - p$.

To train a DNN controller for the model in (9), we follow the approach described in prior work [26]. We sample multiple points from the state space over a horizon T and train a sequence of DNNs, one for each dynamics step (as discretized using the Runge-Kutta method). Once two consecutive DNNs have similar training error,

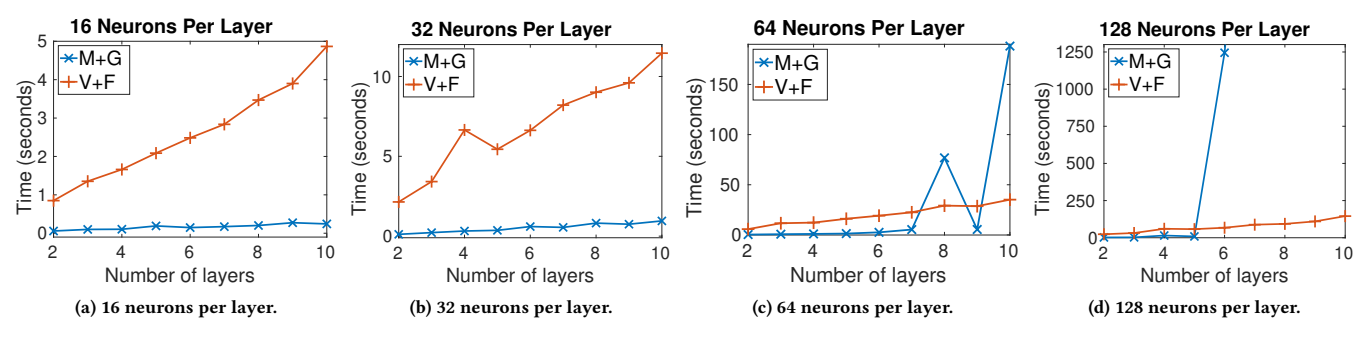


Figure 6: Comparison between the verification times of Verisig+Flow* (V+F) and the MILP-based approach with Gurobi (M+G) for DNNs of increasing size. In each figure, the number of neurons is fixed and number of layers varies from two to 10.

we interrupt training and pick the last DNN as the final controller. The DNN takes a relative state as input and outputs one of eight possible actions (the "bang-bang" strategy implies there are two options per control action). We trained a two-hidden layer tanhbased DNN, with 20 neurons per layer and a linear last layer.

Given the trained DNN controller, we verify the safety property shown in Figure 5. Specifically, the quadrotor is started from an initial condition $(p_X^r(0), p_y^r(0)) \in [-0.05, 0.05] \times [-0.05, 0.05]$ (the other states are initialized at 0) and needs to stay within 0.32m from the planner in order to reach its goal without colliding into obstacles. Similar to the MC case study, we split the initial condition into smaller subsets and verify the property for each subset.

The verification times of Verisig+Flow* for each subset are shown in Table 2. Most cases take less than 30 minutes to verify, which is acceptable for an offline computation. Note that this verification task is harder than MC not because of the larger dimension of the state space but because of the discrete DNN outputs. This means that Verisig+Flow* needs to enumerate and verify all possible paths from the initial set. This process is computationally expensive since the number of paths could grow exponentially with the length of the scenario (set to 30 steps in this case study). One approach to reduce the computation time would be to use the Markov property of dynamical systems and skip states that have been verified previously. We plan to explore this idea as part of future work.

In summary, this section shows that Verisig can verify both safety (avoiding obstacles) and bounded liveness (going up a hill) properties in different and challenging domains. The plant models can be nonlinear systems specified in either discrete or continuous time. The next section shows that Verisig+Flow* also scales well to larger DNNs and is competitive with other approaches for verification of DNN properties in isolation.

6 COMPARISON WITH OTHER DNN VERIFICATION TECHNIQUES

This section complements the Verisig evaluation in Section 5 by analyzing the scalability of the proposed approach. We train DNNs of increasing size on the MC problem and compare the verification times against the times produced by another suggested approach to the verification of sigmoid-based DNNs, namely one using a MILP formulation of the problem [7]. We verify properties about DNNs only (without considering the closed-loop system), since existing approaches cannot be used to argue about the closed-loop system.

As noted in the introduction, the two main classes of DNN verification techniques that have been developed so far are SMT- and MILP-based approaches to the verification of ReLU-based DNNs. Since both of these techniques were developed for piecewise-linear activation functions, neither of them can be directly applied to sigmoid-based DNNs. Yet, it is possible to extend them to sigmoids by bounding the sigmoid from above and below by piecewise-linear functions. In particular, we implement the MILP-based approach for comparison purposes since it can also be used to reason about the reachability of a DNN, similar to Verisig+Flow*.

The encoding of each sigmoid-based neuron into an MILP problem is described in detail in [7]. It makes use of the so called Big M method [33], where conservative upper and lower bounds are derived for each neuron using interval analysis. The encoding uses a binary variable for each linear piece of the approximating function such that when that variable is equal to 1, the inputs are within the bounds of that linear piece (all binary variables have to sum up to 1 in order to enforce that the inputs are within the bounds of exactly one linear piece). Thus, the MILP contains as many binary variables per neuron as there are linear pieces in the approximating function. Finally, one can use Gurobi to solve the MILP and compute a reachable set of the outputs given constraints on the inputs.

To compare the scalability of the two approaches, we trained multiple DNNs on the MC problem by varying the number of layers from two to ten and the number of neurons per layer from 16 to 128. A DNN is assumed to be "trained" if most tested episodes result in a reward of at least 90 – since this is a scalability comparison only, no closed-loop properties were verified. For each trained DNN, we record the time to compute the reachable set of control actions for input constraints $p_0 \in [-0.52, -0.5]$ and $v_0 = 0$ using both Verisig+Flow* and the MILP-based approach. For fair comparison, the two techniques were tuned to have similar approximation error; thus, we used roughly 100 linear pieces to approximate the sigmoid.

The comparison is shown in Figure 6. The MILP-based approach is faster for small networks and for large networks with few layers. As the number of layers is increased, however, the MILP-based approach's runtimes increase exponentially due to the increasing number of binary variables in the MILP. Verisig+Flow*, on the other hand, scales linearly with the number of layers since the same computation is run for each layer (i.e., in each mode). This means that Verisig+Flow* can verify properties about fairly deep

networks; this fact is noteworthy since deeper networks have been shown to learn more efficiently than shallow ones [31].

Another interesting aspect of the behavior of the MILP-based approach can be seen in Figure 6c. The verification time for the nine-layer DNN is much faster than for the eight-layer one, probably due to Gurobi exploiting a corner case in that specific MILP. This suggests that the fast verification times of the MILP-based approach should be treated with caution as it is not known which example can trigger a worst-case behavior. In conclusion, Verisig+Flow* scales linearly and predictably with the number of layers and can be used in a wide range of closed-loop systems with DNN controllers.

7 CONCLUSION AND FUTURE WORK

This paper presented Verisig, a hybrid system approach to verifying safety properties of closed-loop systems with DNN controllers. We showed that the verification problem is decidable for networks with one hidden layer and decidable for general DNNs if Schanuel's conjecture is true. The proposed technique uses the fact that the sigmoid is a solution to a quadratic differential equation, which allows us to transform the DNN into an equivalent hybrid system. Given this transformation, we cast the DNN verification problem into a hybrid system verification problem, which can be solved by existing reachability tools such as Flow*. We evaluated both the applicability and scalability of Verisig+Flow* in two case studies.

For future work, it would be interesting to investigate whether one could use sigmoid-based DNNs to approximate DNNs with other activation functions (with analytically bounded error). This would enable us to verify properties about arbitrary DNNs and would greatly expand the application domain of Verisig.

A second direction for future work is to speed up the verification computation by exploiting the fact that the sigmoid dynamics are monotone and quadratic. Although the proposed technique is already scalable to a wide range of applications, it still makes use of a general-purpose hybrid system verification tool, i.e., Flow*. That is why, developing a specialized sigmoid verification tool might bring significant benefits in terms of scalability and precision.

ACKNOWLEDGMENTS

We thank Xin Chen (University of Dayton, Ohio) for his help with encoding the case studies in Flow*. We also thank Vicenç Rubies Royo (University of California, Berkeley) for sharing and explaining his code on approximating MPCs with DNNs. Last, but not least, we thank Luan Nguyen and Oleg Sokolsky (University of Pennsylvania) for fruitful discussions about the verification technique.

REFERENCES

- US National Highway Traffic Safety Administration. [n. d.]. Investigation PE 16-007. https://static.nhtsa.gov/odi/inv/2016/INCLA-PE16007-7876.pdf.
- [2] R. Alur, C. Courcoubetis, N. Halbwachs, T. A. Henzinger, P. H. Ho, X. Nicollin, A. Olivero, J. Sifakis, and S. Yovine. 1995. The algorithmic analysis of hybrid systems. *Theoretical computer science* 138, 1 (1995), 3–34.
- [3] US National Transportation Safety Board. [n. d.]. Preliminary Report Highway HWY18MH010. https://www.ntsb.gov/investigations/AccidentReports/Reports/HWY18MH010-prelim.pdf.
- [4] X. Chen, E. Ábrahám, and S. Sankaranarayanan. 2013. Flow*: An analyzer for nonlinear hybrid systems. In International Conference on Computer Aided Verification. Springer. 258–263.
- [5] S. Coogan and M. Arcak. 2015. Efficient finite abstraction of mixed monotone systems. In Proceedings of the 18th International Conference on Hybrid Systems: Computation and Control. ACM, 58–67.

- [6] T. Dreossi, A. Donzé, and S. A. Seshia. 2017. Compositional falsification of cyberphysical systems with machine learning components. In NASA Formal Methods Symposium. Springer, 357–372.
- [7] S. Dutta, S. Jha, S. Sankaranarayanan, and A. Tiwari. 2018. Output Range Analysis for Deep Feedforward Neural Networks. In NASA Formal Methods Symposium. Springer, 121–138.
- [8] R. Ehlers. 2017. Formal verification of piece-wise linear feed-forward neural networks. In *International Symposium on Automated Technology for Verification* and Analysis. Springer, 269–286.
- [9] G. Frehse et al. 2011. SpaceEx: Scalable verification of hybrid systems. In International Conference on Computer Aided Verification. 379–395.
- [10] S. Gao, S. Kong, W. Chen, and E. Clarke. 2014. Delta-complete analysis for bounded reachability of hybrid systems. arXiv preprint arXiv:1404.7171 (2014).
- [11] I. Goodfellow, Y. Bengio, A. Courville, and Y. Bengio. 2016. Deep learning. Vol. 1. MIT press Cambridge.
- [12] M. Hertneck, J. Köhler, S. Trimpe, and F. Allgöwer. 2018. Learning an approximate model predictive controller with guarantees. *IEEE Control Systems Letters* 2, 3 (2018), 543–548.
- [13] K. Hornik, M. Stinchcombe, and H. White. 1989. Multilayer feedforward networks are universal approximators. *Neural networks* 2, 5 (1989), 359–366.
- [14] K. D. Julian, J. Lopez, J. S. Brush, M. P. Owen, and M. J. Kochenderfer. 2016. Policy compression for aircraft collision avoidance systems. In *Digital Avionics Systems Conference (DASC)*, 2016 IEEE/AIAA 35th. IEEE, 1–10.
- [15] G. Katz, C. Barrett, D. L. Dill, K. Julian, and M. J. Kochenderfer. 2017. Reluplex: An efficient SMT solver for verifying deep neural networks. In *International Conference on Computer Aided Verification*. Springer, 97–117.
- [16] M. J. Kearns and U. Vazirani. 1994. An introduction to computational learning theory. MIT press.
- [17] S. Kong, S. Gao, W. Chen, and E. Clarke. 2015. dReach: δ-reachability analysis for hybrid systems. In International Conference on TOOLS and Algorithms for the Construction and Analysis of Systems. Springer, 200–205.
- [18] G. Lafferriere, G. J. Pappas, and S. Yovine. 1999. A new class of decidable hybrid systems. In *International Workshop on Hybrid Systems: Computation and Control*. 137–151.
- [19] T. P. Lillicrap, J. J. Hunt, A. Pritzel, N. Heess, T. Erez, Y. Tassa, D. Silver, and D. Wierstra. 2015. Continuous control with deep reinforcement learning. arXiv preprint arXiv:1509.02971 (2015).
- [20] V. Mnih et al. 2015. Human-level control through deep reinforcement learning. Nature 518, 7540 (2015), 529.
- [21] M. Mohri, A. Rostamizadeh, and A. Talwalkar. 2012. Foundations of machine learning. MIT press.
- [22] L. D. Moura and N. Bjørner. 2008. Z3: An efficient SMT solver. In International conference on Tools and Algorithms for the Construction and Analysis of Systems. Springer, 337–340.
- [23] OpenAI. [n. d.]. OpenAI Gym. https://gym.openai.com.
- [24] Gurobi Optimization. [n. d.]. Gurobi Optimizer. https://gurobi.com.
- [25] L. Pulina and A. Tacchella. 2010. An abstraction-refinement approach to verification of artificial neural networks. In *International Conference on Computer Aided* Verification. Springer, 243–257.
- [26] V. R. Royo, D. Fridovich-Keil, S. Herbert, and C. J. Tomlin. 2018. Classification-based Approximate Reachability with Guarantees Applied to Safe Trajectory Tracking. arXiv preprint arXiv:1803.03237 (2018).
- [27] D. Silver, A. Huang, C. J. Maddison, A. Guez, et al. 2016. Mastering the game of Go with deep neural networks and tree search. *nature* 529, 7587 (2016), 484.
- [28] C. Szegedy, W. Zaremba, I. Sutskever, J. Bruna, D. Erhan, et al. 2013. Intriguing properties of neural networks. arXiv preprint arXiv:1312.6199 (2013).
- [29] Y. Taigman, M. Yang, M. Ranzato, and L. Wolf. 2014. Deepface: Closing the gap to human-level performance in face verification. In Proceedings of the IEEE conference on computer vision and pattern recognition. 1701–1708.
- [30] A. Tarski. 1998. A decision method for elementary algebra and geometry. In Quantifier elimination and cylindrical algebraic decomposition. Springer, 24–84.
- [31] M. Telgarsky. 2016. Benefits of depth in neural networks. arXiv preprint arXiv:1602.04485 (2016).
- [32] C. E. Tuncali, H. Ito, J. Kapinski, and J. V. Deshmukh. 2018. Reasoning about safety of learning-enabled components in autonomous cyber-physical systems. In 2018 55th ACM/ESDA/IEEE Design Automation Conference (DAC). IEEE, 1–6.
- [33] R. J. Vanderbei et al. 2015. Linear programming. Springer.
- [34] A. J. Wilkie. 1997. Schanuel's conjecture and the decidability of the real exponential field. In Algebraic Model Theory. Springer, 223–230.
- [35] W. Xiang et al. 2018. Verification for Machine Learning, Autonomy, and Neural Networks Survey. arXiv preprint arXiv:1810.01989 (2018).
- [36] W. Xiang, H. D. Tran, and T. T. Johnson. 2017. Output reachable set estimation and verification for multi-layer neural networks. arXiv preprint arXiv:1708.03322 (2017).
- [37] C. Zhang, S. Bengio, M. Hardt, B. Recht, and O. Vinyals. 2016. Understanding deep learning requires rethinking generalization. arXiv preprint arXiv:1611.03530 (2016).